

Densely tracking sequences of 3D face scans

Huaxiong DING

Ecole Centrale de LYON

huaxiong.ding@ec-lyon.fr

Liming Chen

Ecole Centrale de LYON

liming.chen@ec-lyon.fr

Abstract

3D face dense tracking aims to find dense inter-frame correspondences in a sequence of 3D face scans and constitutes a powerful tool for many face analysis tasks, e.g., 3D dynamic facial expression analysis. The majority of the existing methods just fit a 3D face surface or model to a 3D target surface without considering temporal information between frames. In this paper, we propose a novel method for densely tracking sequences of 3D face scans, which extends the non-rigid ICP algorithm by adding a novel specific criterion for temporal information. A novel fitting framework is presented for automatically tracking a full sequence of 3D face scans. The results of experiments carried out on the BU4D-FE database are promising, showing that the proposed algorithm outperforms state-of-the-art algorithms for 3D face dense tracking.

1. Introduction

In facial behavior analysis, especially facial expression recognition, the use of 3D face scans is regarded as a promising solution [20]. Because compared with 2D images based system, it is relatively insensitive to facial pose changes, illumination conditions, and other changes in facial appearance like facial cosmetics. Moreover, a 3D facial scan contains more information displayed by face than a single-view 2D image, as it can additionally record out-of-plane changes of the face surface. Thus, 3D face based systems for facial expression analysis have attracted many researchers in the past decades.

Facial expression is naturally caused by the motions of facial muscles beneath the skin of the face. Consequently, the use of dynamic face sequences is thought to be more reasonable and promising than only using a static image, since it can encode both spatial and temporal deformation information at the same time. However, to capture a sequence of 3D face scans is indeed much difficult than capturing a 2D video. But fortunately, recent advances in 3D face data acquisition (*i.e.* structured light scanning [7], photometric stereo [23] and multi-view stereo [6]) have made it

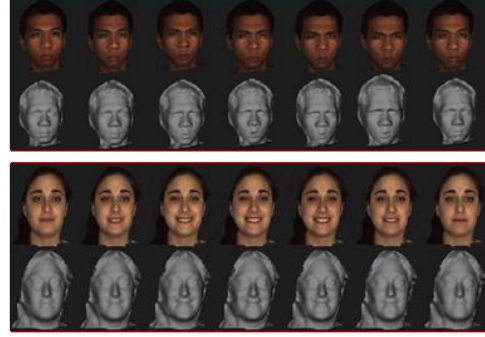


Figure 1. Examples from 3D dynamic facial expression databases BU4D-FE.

a feasible task. As a result, a number of dynamic 3D face databases have been proposed for this issue, like BU4D-FE [24] and BP4D-spontaneous [25], as shown in Fig. 1. More recently, with the popular use of low-cost range sensors, such as Kinect, facial expression analysis using low resolution dynamic 3D data has also attracted the attention.

To extract features of motions in the same location or region on the different frames of sequences, accurate alignment and tracking methods become very important for facial expression systems. Normally, 3D face fitting, which aims at finding an optimal warp between a template surface (*i.e.* mesh or cloud points) and a target surface, is a key step to solve this issue. According to the number of correspondent points, the majority of existing methods in 3D face fitting can be divided into two categories: sparse vs. dense. Unlike the former which only locates a set of fiducial points (*e.g.* eye corner and nose tip), the latter needs to find a mapping from each point in the template onto the target. Obviously, dense fitting is more challenging but more attractive, as it is able to grab variations of 3D face scans more accurately. Meanwhile, another advantage of dense fitting is that it is easy to train and construct a statistical model based on the fitted results and the established correspondences.

Dense face fitting has many applications in 3D face analysis, as an accurate fitting algorithm is able to benefit facial recognition [17, 13] and facial expression recogni-

tion [3, 20, 19]. Normally, 3D dense fitting can help align face scans and model facial expressions in the majority of existing works [20]. More recently, since 3D dense tracking can provide dense trajectories through sequences of facial expression variations, improving facial expression recognition using dense trajectory is another research trend [1].

Reviewing the development in 3D face dense fitting, various efforts have been made for this issue, such as free-form deformations (FFDs) [18], statistical models [3, 16], non-rigid ICP based algorithms [4, 9], harmonic maps [21], and conformal mappings [11]. However, the majority of existing methods is initially proposed for static face scans fitting, which means it just maps a template surface or model to a target surface independently. Most of them disregard temporal information between frames when they are used to fit a sequence rather than a single face scan.

In this paper, we address the problem of 3D dense tracking and propose a novel method for tracking sequences of 3D face scans. The contributions are as follows: Firstly, we improve the non-rigid Iterative Closest Point (ICP) algorithm by introducing a specific criterion with respect to temporal information between frames. Besides it, a novel dynamic framework is proposed to automatically fit full sequences of 3D face scans iteratively. Moreover, we propose a joint 2D and 3D framework to detect facial landmarks on 3D face scans. Furthermore, we present several techniques for non-rigid ICP to improve the convergence and achieve a good initialization, including employing a 3D identity/expression separated morphable model to generate a template surface as a rough shape estimation and introducing a variant of ICP with a scale factor to automatically align two surfaces and rescale them into the same range.

The rest of the paper is organized as follows. Section 2 reviews 3D dense fitting and tracking methods. Section 3 presents in detail the proposed method including preprocessing, landmark detection and fitting procedure. Section 4 shows the fitting results and discusses some quantitative analysis in the experiments. Finally, Section 5 concludes this paper.

2. Related works

Many efforts have been made to tackle the problem of 3D dense fitting, for example, morphable models [16, 3], non-rigid ICP based algorithms [2, 4, 9], harmonic maps [21] and conformal mappings [11]. In this section, we introduce different kinds of 3D face dense fitting algorithm and discuss their advantages and disadvantages respectively.

Harmonic maps were firstly introduced by Wang *et al.* [21] to find dense correspondences between 3D face surfaces. The main idea of the proposed method is using harmonic maps to project each surface to the canonical unit disk on the plane with minimal stretching energy and bounded angle distortion. A sparse set of easily detectable

motion representative feature corners on the disks is employed to find dense correspondence on 2D disk. Conformal mapping proposed by Gu *et al.* [11] also projects 3D surface into a 2D plane, but it preserves angles between edges of the mesh in the projection. The dense correspondence on 2D disk is found by minimizing the matching function, which combines the optimal Mbius transformation and the global matching function (OMGMF). Both harmonic map and conformal mapping are one-to-one, so the dense correspondences on the 3D mesh can be established once the set of correspondences on the 2D disks has been calculated. Overall, the advantage of conformal mapping is that it can provide very accurate dense correspondence, but it requires meshes with high quality, needs a prior knowledge of boundaries of surfaces, and it is very computationally expensive.

3D morphable models (3DMMs) is a very useful technique that has been exploited in 3D fitting and alignment. The fitting function normally allows rigid deformations, such as rotation and translation, from the mean shape, and the non-rigid transformation is defined as a linear combination of basis vectors. Munoz *et al.* [16] proposed a 3DMMs based method for tracking 2D image sequences, in which the efficiency is achieved by factoring the Jacobian and Hessian matrices appearing in the GaussNewton optimization into the multiplication of a constant matrix depending on target structure and texture, and a varying matrix that depends on the target motion and deformation parameters. Amberg *et al.* [3] proposed an iterative method for 3D face dense fitting, which used an identity/expression separated 3D Morphable Model to fit the correspondences found by ICP algorithm. Generally, 3DMMs based fitting method can be very fast, and it is also robust to noise in the raw input. However, since the non-linearity of 3DMMs is ensured by PCA decomposition basis, the fitting results are restricted by variations of shape data used to build it. For example, a 3DMM established with all faces with neutral expression is hard to fit a target face with high-intensity expression. And besides, the complexity of local geometry detail of the fitting results also indeed relies on the number of PCA basis.

Iterative close point (ICP) is another algorithm widely employed for 3D face alignment, which fits a template surface to a target surface. Firstly, all points or a subset of points in the template are designed to find a correspondent point in the target with the closest distance. Then it wraps the template surface into the target surface using the deformation computed from the correspondences. The deformation of traditional ICP is rigid. Some algorithms [2, 4, 9] that extend ICP methods to non-rigid deformations have been proposed for 3D dense fitting. Amberg *et al.* [4] defined an affine deformation matrix for each vertex in the template, and used a stiffness term to regularize the non-rigid deformation. More recently, Cheng *et al.* [9] proposed

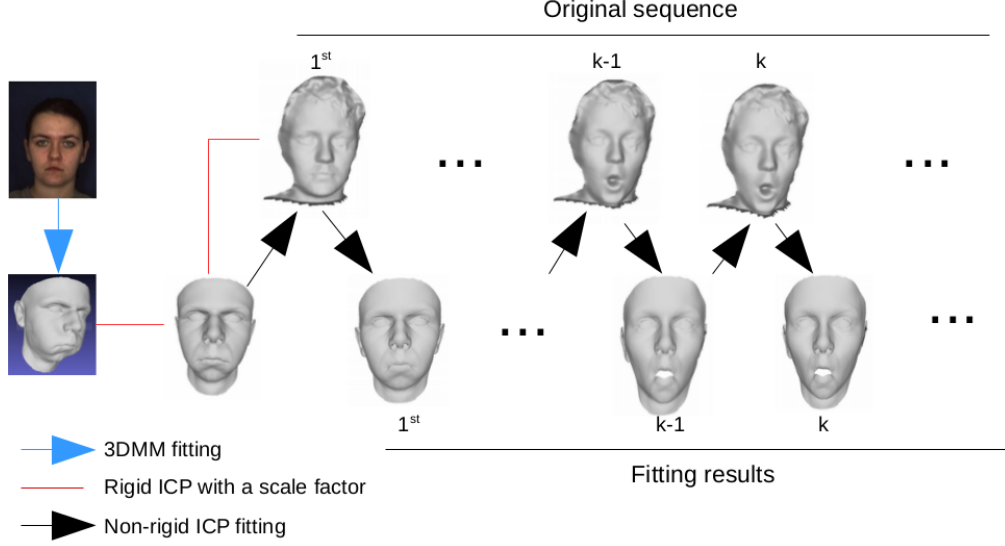


Figure 2. Overview of the proposed framework for automatically densely fitting sequences of 3D face scans

a novel method additionally introducing the statistical prior as an extra constraint on the fitting procedure of non-rigid ICP, in which a face mesh is first divided into several regions by annotated model of the face (AFM) [12], then on each subdivided region, a combination of a linear statistical model and the non-rigid ICP is employed to fit this local region. However, non-rigid ICP is able to handle pose variations, occlusions, and even missing data. But it is a little sensitive to initialization and vulnerable to noisy data as it will fit to all points.

3. Proposed Method

In this section, we present in detail the proposed method that is able to automatically densely track sequences of 3D face scans.

Fig. 2 shows an overview of the framework employed in the proposed method. First of all, a set of spatial facial landmarks is located by a joint 2D and 3D face framework, which is used as a prior knowledge for both 3DMMs and ICP fitting. Meanwhile, considering that a good initialization can indeed boost the convergence of ICP-like algorithms, we use a 3D morphable model to fit the 1_{st} frame of the sequences and adapt the fitted 3D face as a rough shape estimation of 1_{st} frame, which will play a role of the template surface in the ICP fitting process. Normally, the coordinates of the fitted 3D face and the target surface are not in the range. Therefore, a variant of rigid ICP with a scale factor is employed to coarsely align and re-scale two surfaces to be fitted. After we have a coarse alignment of that two surface, the proposed novel variant of non-rigid ICP algorithm is used to refine local deformations. Iteratively, given the fitting results of the previous frame, we use

it as the template surface to fit the face scan in the current frame. Finally, we repeat the rule to fit a whole sequence until it ends.

3.1. Joint 2D and 3D facial landmark detection

Due to the importance of correspondence for the ICP-like algorithm, our method reasonably relies on facial landmarks extracted from both two face surfaces to be fitted, which are treated as a solid correspondence to guide the convergence and restrict the large global deformations.

Benefit from the recent breakthrough of the 2D face landmark detection algorithm, detecting face landmarks on texture images has become more reliable. Here, we present a framework as described in [15] using 2D landmark localization algorithm to help locate face landmarks on the 3D mesh. More specifically, as shown in Fig. 3, a 3D face scan with texture map is firstly projected into a 2D plane using z-buffer algorithm. Then a landmark fitting algorithm based on an ensemble of regression trees [14] is used to locate landmarks on the projected 2D image. These 2D landmarks are further transferred to 3D texture face space by the inverse of the above projection. Since the one-to-one correspondence between 3D texture and 2D texture is approximately preserved during the projection mapping, 3D landmarks can be directly determined by the one-to-one correspondence between 3D texture and 3D geometry of the 3D face model.

3.2. 3D Morphable model fitting

3D morphable model originally proposed by [8] is an effective method to describe 3D face space with the PCA. As introduced previously, the non-linearity of 3DMMs is re-

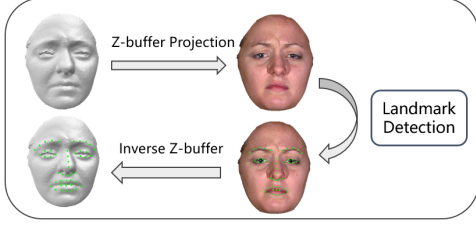


Figure 3. The joint 2D and 3D face landmark localization framework.

stricted by the combination of PCA basis vectors. Thus, to better fit the face with various expressions, we introduce an identity/expression separated morphable model [26] to handle shape deformations caused by variations of facial expression, e.g. mouth open, as shown in Fig. 4.

$$S(\alpha_{id}, \alpha_{exp}) = \bar{S} + A_{id}\alpha_{id} + A_{exp}\alpha_{exp} \quad (1)$$

where S is the 3D face, \bar{S} is the mean shape, A_{id} represents the identity component trained on the offset between neutral face scans and the mean shape and α_{id} is the identity coefficient, M_{exp} represents the expression component trained on the offset between expression scans and neutral scans and α_{exp} is the expression coefficient.

Then the 3D face scan is projected into 2D plane:

$$s_{2d} = fPR(S + t_{3d}) \quad (2)$$

where s_{2d} is the projected image on image plane, f is the scale factor, P is defined as the orthographic projection matrix, R is the rotation matrix on 3D space and t_{3d} is the translation matrix.

The fitting process is to minimize the difference between projected 2D image and the image to be fitted.

$$\arg \min_{f, R, t_{3d}, \alpha_{3d}, \alpha_{exp}} \|s_{2d_{truth}} - s_{2d}\| \quad (3)$$

3.3. ICP registration with a scale factor

Given the 3D face fitted by 3DMMs, referred as the template surface, we need further align it to the target surface that is a frame of the 3D dynamic face sequence. Actually, the coordinates of vertices in the template are not in the same range as that of vertices in the target, as shown in Fig. 4. To well solve this issue, we use a variant of rigid ICP equipped with a scale factor [27]. Meanwhile, since facial landmarks have been firstly located on both two surfaces, we employ all pairs of landmarks as the correspondences used to calculate deformations in the process of ICP.

The fitting function minimizes the difference when we warp points a_i in the template to points b_j in the target.

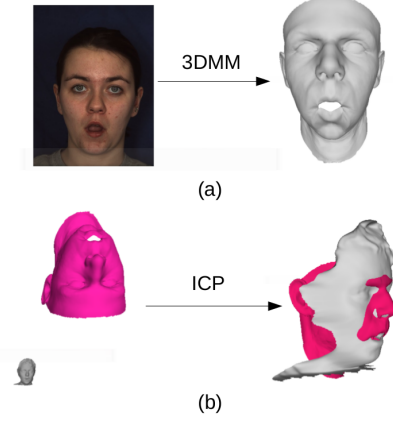


Figure 4. (a). A 3D face is fitted by a 3D morphable model from 2D texture images. (b). An ICP registration with a scale factor is used to align and re-scale two face surfaces.

$$(R^*, t^*, s^*) = \arg \min_{R, t, s} \sum_{(i,j) \in C} \|b_j - sRa_i - t\|^2 \quad (4)$$

where R is the rotation matrix, t is the translation vector, s is the scale factor.

To solve this function, the center of mass \bar{a} of the selected data points and the center of mass \bar{b} of the corresponding model points are firstly computed according to

$$\bar{a} = \frac{1}{|C|} \sum_{(i,j) \in C} a_i, \quad \bar{b} = \frac{1}{|C|} \sum_{(i,j) \in C} b_i \quad (5)$$

This problem is solved by computing the SVD of the matrix

$$K = \sum_{(i,j) \in C} (b_j - \bar{b})(a_i - \bar{a})^T = UDV^T \quad (6)$$

where $R^* = UV^T$ that is regarded as an approximation of the rotation matrix. Then the scale factor s^* can be estimated by

$$s^* = \frac{\sum_{(i,j) \in C} \tilde{b}_j^T \tilde{a}_i}{\sum_{(i,j) \in C} \tilde{a}_i^T \tilde{a}_i} \quad (7)$$

where

$$\tilde{b}_j = (b_j - \bar{b}), \quad \tilde{a}_i = R^*(a_i - \bar{a}) \quad (8)$$

Finally, the translation vector t^* can be computed by $t^* = \bar{b} - s^* R^* \bar{a}$.

3.4. Non-rigid ICP with motion information

In this section, we present in detail the proposed non-rigid ICP algorithm that mainly extends the work [4] with a novel temporal information regularization.

We denote the template surface $\mathcal{S} = (\mathcal{V}, \mathcal{E})$, with a set of n vertices \mathcal{V} and a set of m edges \mathcal{E} . The target surface is denoted as \mathcal{T} . The goal of fitting is to find an optimal mapping $\mathcal{V}(X)$ wrapping the template into the target while preserving the topology structure.

More specifically, for each vertex in the template, we define a 3×4 affine deformation matrix X_i to allow the non-rigid transformation. Therefore, we need to find an optimal $4n \times 3$ matrix X to minimize the cost function with multiple regularizations in the fitting process.

$$X := [X_1 \cdots X_n]^T \quad (9)$$

3.4.1 Cost function

The cost function used in this paper is similar to the one defined in [4]. The difference is, that we add a new specific item with respect to the motion history in previous frames to meet the acquirement of tracking a sequence. Besides it, since we have already automatically located facial landmarks on both two surfaces, we use the item measuring the difference from the set of landmarks to guide the convergence and restrict illegal deformations, unlike [4] uses manually annotated landmarks.

The proposed cost function consists of four items: a vertex distance item, a stiffness term, a landmark distance item, and a motion history item.

Vertex distance item: The item measures the Euclidean distance between source vertex v_i and its closest vertex u_i in the target surface.

$$E_d(X) := \sum_{v_i \in \mathcal{V}} w_i \|X_i v_i - u_i\|^2 \quad (10)$$

where w_i is a coefficient to weight the reliability of correspondences. The robustness is achieved by setting w_i to zero, if it can not find the corresponding vertex in the case of missing data.

Stiffness item: The item penalizes the differences between the transformation matrices assigned to neighboring vertices that belong to the same edge. In fact, this item is employed to smooth the deformation and avoid abrupt shape changes.

$$E_s(X) := \sum_{\{i,j\} \in \mathcal{E}} \|(X_i - X_j)G\|_F^2 \quad (11)$$

where $G := \text{diag}(1, 1, 1, \lambda)$, λ is used to weight influences of the rotational and skew part against that of the translational part in the deformation.

Landmark item: Similar to the regularization on vertices, the item measures the distance between all pairs of landmark correspondences $\mathcal{L} = \{(v_1, l_1), \dots, (v_k, l_k)\}$.

$$E_l(X) := \sum_{(v_i, l_i) \in \mathcal{L}} \|X_i v_i - l_i\|^2 \quad (12)$$

Motion history item: As introduced previously, the one-to-one correspondences are naturally established in the set of fitted face scans. Therefore, for each vertex, we could obtain a motion trajectory through a sequence. Based on techniques of trajectory analysis, an approximation of the position of a vertex in the current frame can be estimated according to the positions of that point in the previous frames.

Following this idea, we could generate a face surface using these estimated coordinates of vertices, then use it as a regularization factor to guide the transformation in the fitting process.

The definition of the item is as follows:

$$v_i^{k*} = f(v_i^1, \dots, v_i^{k-1}) \quad (13)$$

where v_i^{k*} is a estimated vertex, and f is a trajectory estimator. In the experiments, we only use the classic Kalman estimator as it is easy to be implemented. Different kinds of more complex trajectory estimators can be found in [5, 10].

Similarly, the item also take the distances of vertices as the measurement.

$$E_m(X) := \sum_{v_i \in \mathcal{V}} \|X_i v_i - v_i^{k*}\|^2 \quad (14)$$

Cost function: The full cost function is a weighted sum of these terms:

$$E(X) := E_d(X) + \alpha E_s(X) + \beta E_l(X) + \gamma E_m(X) \quad (15)$$

Here, α is the stiffness weight that influences the flexibility of the template, β weights the importance of facial landmarks, and γ is related to the influence of motion information.

3.4.2 Parameters optimization

We follow a similar framework as [4] to find the optimal affine transformation by minimizing the cost function iteratively. For each iteration, the preliminary correspondences are firstly determined. Then, based on the preliminary correspondences, we calculate the optimal transformation parameters for the current iteration. The transformed template and the target will lead to finding the new correspondences for next iteration. This process is repeated until it converges, as shown in Algo. 1.

Actually, once the correspondences are fixed, the cost function can be transferred to a sparse quadratic system

Algorithm 1 Non-rigid ICP fitting algorithm

Require:

Two 3D face meshes: template \mathcal{V} and target \mathcal{T}

- 1: Initialize affine parameters X^0
- 2: Choose a set of stiffness coefficients $\{\alpha^1, \dots, \alpha^n\}$, $\alpha_i > \alpha_{i+1}$, landmark coefficients $\{\beta^1, \dots, \beta^n\}$, $\beta_i > \beta_{i+1}$ and motion coefficients $\{\gamma^1, \dots, \gamma^n\}$, $\gamma_i > \gamma_{i+1}$.
- 3: **for** each $\alpha_i, \beta_i, \gamma_i$ **do**
- 4: **while** $\|X_j - X_{j-1}\| > \varepsilon$ **do**
- 5: Find preliminary correspondences for $\mathcal{V}(X)$
- 6: Calculate optimal local affine transform X_j
- 7: based on correspondences, α_i, β_i and γ_i
- 8: **end while**
- 9: **end for**
- 10: **return** X

which can be minimized exactly. More specially, in order to differentiate the formulation, we rewrite items of cost function into canonical form. For the vertex distance item, we swap the positions of the unknowns and the fixed vertices:

$$E_d(X) := \|W(DX - U)\|_F^2 \quad (16)$$

Where $W := \text{diag}(w_1, \dots, w_n)$, D is a sparse matrix mapping the $4n \times 3$ matrix of unknowns X onto displaced source vertices.

For the stiffness item, we define a node-arc incidence matrix M . If edge r connects the vertices (i, j) and $i < j$, the nonzero entries of M in row r are $M_{ri} = 1$ and $M_{rj} = 1$. Then the item can be rewritten as:

$$E_s(X) := \|(M \otimes G)X\|_F^2 \quad (17)$$

Similarly, the rest two item can also be rewritten in the form of

$$E_l(X) := \|D_L X - U_L\|_F^2 \quad (18)$$

$$E_m(X) := \|DX - U_m\|_F^2 \quad (19)$$

Now, the original cost function becomes a quadratic function:

$$\begin{aligned}
E(X) &= \left\| \begin{bmatrix} WD \\ \alpha M \otimes G \\ \beta D_L \\ \gamma D \end{bmatrix} X - \begin{bmatrix} WU \\ 0 \\ \beta U_L \\ \gamma U_m \end{bmatrix} \right\|_F^2 \\
&= \|AX - B\|_F^2
\end{aligned} \quad (20)$$

which is a typical linear least square problem. And $E(X)$ takes on its minimum at $X = (A^T A)^{-1} A^T B$. Thus, For each iteration, given fixed correspondences and coefficients, we could determine the optimal deformation quickly.

4. Experimental Evaluation

In this section, we present our experiments and discuss the experimental results in detail.

4.1. Database

BU4D-FE [24] is a high-resolution 3D dynamic facial expression database, which contains facial expression sequences captured from 101 subjects. For each subject, there are six model sequences showing six prototypic facial expressions (anger, disgust, happiness, fear, sadness, and surprise), respectively. Each expression sequence contains about 100 frames. Each 3D model is equipped with a high-resolution texture map. Some examples have been shown in Fig. 1

4.2. Experimental setup

The experiments are carried out on a subset of BU4D-FE database. The sequences of 20 subjects are selected to evaluate the proposed method. Since ICP needs to find correspondences for each point on surfaces, several pre-processings have been applied to remove noise points, such as spikes and small isolated pieces, for achieving a robust performance.

Now, we introduce some details for implementation and present parameters that we used in the experiments. For landmark detection, we employ the algorithm proposed in [14] and locate totally 51 landmarks on the face. In rigid registration, all the surfaces are aligned and re-scaled into a cube $[0, 1]$ to avoid too large value in the computation. In the stage of Non-rigid ICP, once the correspondences have been established by the closest distance, another criterion is applied to increase the reliability, which is achieved by dropping correspondences if the angle between normal directions of two correspondent points is large than $\frac{\pi}{4}$. Finally, in the cost function of non-rigid ICP, α and β vary from 100 to 10 with a step 10, while γ varies from 5 to 0.5 with a step 0.5;

To evaluate the proposed method and compare its fitting result with the state of the art algorithm, we introduce two methods as the baselines. The first method is proposed by [4], referred as NICP, based on which we develop our proposed method. Since 3DMM have been widely used in modeling 3D facial expressions, and even in dense tracking [16], we adapt the 3DMM fitting as our second method for comparison.

4.3. Quantitative analysis

Firstly, to measure the quality of registration, we propose a method based on facial landmarks. More specially, if we have already located facial landmarks on all 3D face scans, we could extract local geometry properties, such coordinates and normal directions, in an n -ring region around

Method	Mean Error (coords $\times 10^{-3}$)	Mean Error (normals)
3DMM	11.3	0.41
NCIP	9.9	0.32
Our Method	8.6	0.31

Table 1. Average error of local geometry properties computed from regions around landmarks.

facial landmarks. Then the difference of extracted geometry properties between the fitting result and the target surface is regarded as the measurement of the registration quality.

Given a set of landmark $\{(v_1, l_1), \dots, (v_k, l_k)\}$, $f(x)$ represents the average value of local geometry properties of regions around the landmark x .

$$measurement := \frac{1}{k} \sum_{i=1..k} D(f(v_i), f(l_i)) \quad (21)$$

where D indicates the Euclidean distance for coordinates, and the angle for normal directions.

Table 1 shows the performance measures of the three fitting methods. We can observe that both two non-rigid ICP based methods outperform 3DMM based fitting algorithm. We think the principle reason to the failure of 3DMM is that the non-linearity of 3DMM is limited by its PCA components and it can not capture out-of-plane changes since it fits 2D images.

However, our method clearly outperforms NCIP in term of coordinate error, which proves that the use of motion information can indeed improve the accuracy and robustness of the fitting results. As a result, it is able to provide more stable dense trajectories for 3D dynamic expression analysis. Meanwhile, its error of normals is still slightly lower than that of NCIP, showing the effectiveness of proposed framework.

4.4. Visualization of fitting results

We show some fitting results with the different intensity of expressions in Fig. 5, from which we can observe that the proposed model fits 3D face much better than 3DMM. Actually, the mouth open is still a challenge for most of the fitting algorithm. The surface of 3D faces fitted by 3DMM is uneven, especially in the region around the mouth, that may be caused by the limitation of non-linearity as we discussed previously. The 3D faces fitted by the proposed method display more details, such as eyelids in a smooth surface. Meanwhile, it is able to capture the deformation of mouth caused by variations of expressions accurately, which also demonstrates the power of the proposed method.

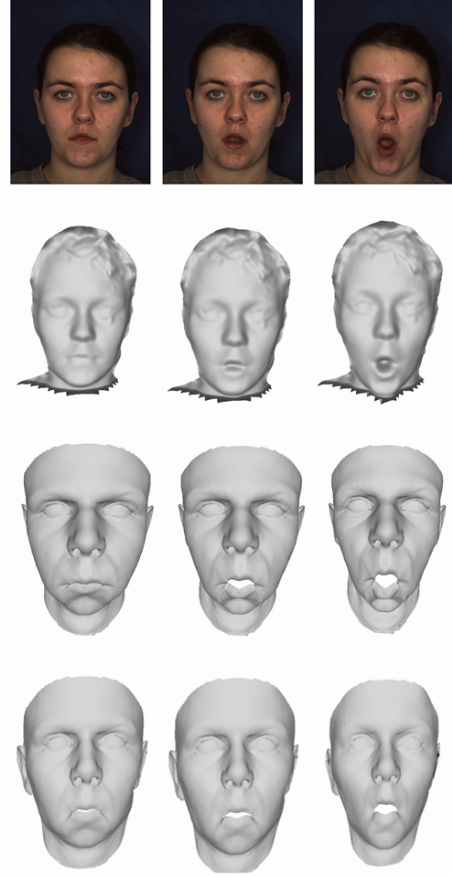


Figure 5. Fitting results for scans with different intensity of expressions from 3D dynamic facial expression databases BU4D-FE. The 1st row presents original texture images and the 2nd row shows original meshes. the 3rd row is the fitting result of 3DMM and the 4th row presents the fitting results of our method.

5. Conclusion and Future Work

In this paper, we tackle the issue of 3D dense tracking and propose a novel framework that is able to densely track the sequences of 3D face scans. The techniques employed in the fitting process to achieve robust results are introduced in detail, including landmark detection, 3DMM fitting, and two-stage ICP registration. To satisfy the terms of dense tracking, we extend the non-rigid ICP by taking into a new criterion into motion information. The experimental results prove that the proposed method is promising to solve this issue.

The family of ICP algorithm relies heavily on the correspondence establishing, which mostly determines the convergence. In this paper, we find the correspondences between two surfaces only using geometry information, such as coordinates and normal directions. Since 3D face scans

are usually along with the texture map, to make use of texture information, the proposed methods [22] designed for finding correspondences on 2D images can be integrated in the future.

This work was supported in part by the French Research Agency, l'Agence Nationale de Recherche (ANR), through the Jemime project (N^ocontract ANR-13-CORD-0004-02), the Biofence project (N^ocontract ANR-13-INSE-0004-02) and the PUF 4D Vision project funded by the Partner University Foundation.

References

- [1] S. Afshar and A. Ali Salah. Facial expression recognition in the wild using improved dense trajectories and fisher vector encoding. In *Proceedings of the IEEE Conference on Computer Vision and Pattern Recognition Workshops*, pages 66–74, 2016.
- [2] B. Allen, B. Curless, and Z. Popović. The space of human body shapes: reconstruction and parameterization from range scans. In *ACM transactions on graphics (TOG)*, volume 22, pages 587–594. ACM, 2003.
- [3] B. Amberg, R. Knothe, and T. Vetter. Expression invariant 3d face recognition with a morphable model. In *Automatic Face & Gesture Recognition, 2008. FG'08. 8th IEEE International Conference on*, pages 1–6. IEEE, 2008.
- [4] B. Amberg, S. Romdhani, and T. Vetter. Optimal step non-rigid icp algorithms for surface registration. In *Computer Vision and Pattern Recognition, 2007. CVPR'07. IEEE Conference on*, pages 1–8. IEEE, 2007.
- [5] T. D. Barfoot, C. H. Tong, and S. Särkkä. Batch continuous-time trajectory estimation as exactly sparse gaussian process regression. In *Robotics: Science and Systems*. Citeseer, 2014.
- [6] T. Beeler, B. Bickel, P. Beardsley, B. Sumner, and M. Gross. High-quality single-shot capture of facial geometry. In *ACM Transactions on Graphics (ToG)*, volume 29, page 40. ACM, 2010.
- [7] C. Beumier and M. Achery. 3d facial surface acquisition by structured light. In *International Workshop on Synthetic-Natural Hybrid Coding and Three Dimensional Imaging*, pages 103–106, 1999.
- [8] V. Blanz and T. Vetter. A morphable model for the synthesis of 3d faces. In *Proceedings of the 26th annual conference on Computer graphics and interactive techniques*, pages 187–194. ACM Press/Addison-Wesley Publishing Co., 1999.
- [9] S. Cheng, I. Marras, S. Zafeiriou, and M. Pantic. Statistical non-rigid icp algorithm and its application to 3d face alignment. *Image and Vision Computing*, 2016.
- [10] J. Gibson and O. Marques. Optical flow and trajectory estimation methods. *SpringerBriefs in computer science*, 2016.
- [11] X. D. Gu and S.-T. Yau. *Computational conformal geometry*. International Press Somerville, Mass, USA, 2008.
- [12] I. A. Kakadiaris, G. Passalis, T. Theoharis, G. Toderici, I. Konstantinidis, and N. Murtuza. Multimodal face recognition: Combination of geometry with physiological information. In *Computer Vision and Pattern Recognition, 2005. CVPR 2005. IEEE Computer Society Conference on*, volume 2, pages 1022–1029. IEEE, 2005.
- [13] I. A. Kakadiaris, G. Passalis, G. Toderici, M. N. Murtuza, Y. Lu, N. Karampatziakis, and T. Theoharis. Three-dimensional face recognition in the presence of facial expressions: An annotated deformable model approach. *IEEE Transactions on Pattern Analysis and Machine Intelligence*, 29(4), 2007.
- [14] V. Kazemi and J. Sullivan. One millisecond face alignment with an ensemble of regression trees. In *Proceedings of the IEEE Conference on Computer Vision and Pattern Recognition*, pages 1867–1874, 2014.
- [15] H. Li, H. Ding, D. Huang, Y. Wang, X. Zhao, J.-M. Morvan, and L. Chen. An efficient multimodal 2d+ 3d feature-based approach to automatic facial expression recognition. *Computer Vision and Image Understanding*, 140:83–92, 2015.
- [16] E. Munoz, J. M. Buenaposada, and L. Baumela. A direct approach for efficiently tracking with 3d morphable models. In *Computer Vision, 2009 IEEE 12th International Conference on*, pages 1615–1622. IEEE, 2009.
- [17] G. Passalis, I. A. Kakadiaris, and T. Theoharis. Intraclass retrieval of nonrigid 3d objects: Application to face recognition. *IEEE Transactions on Pattern Analysis and Machine Intelligence*, 29(2):218–229, 2007.
- [18] G. Sandbach, S. Zafeiriou, M. Pantic, and D. Rueckert. A dynamic approach to the recognition of 3d facial expressions and their temporal models. In *Automatic Face & Gesture Recognition and Workshops (FG 2011), 2011 IEEE International Conference on*, pages 406–413. IEEE, 2011.
- [19] G. Sandbach, S. Zafeiriou, M. Pantic, and D. Rueckert. Recognition of 3d facial expression dynamics. *Image and Vision Computing*, 30(10):762–773, 2012.
- [20] G. Sandbach, S. Zafeiriou, M. Pantic, and L. Yin. Static and dynamic 3d facial expression recognition: A comprehensive survey. *Image and Vision Computing*, 30(10):683–697, 2012.
- [21] Y. Wang, M. Gupta, S. Zhang, S. Wang, X. Gu, D. Samaras, and P. Huang. High resolution tracking of non-rigid motion of densely sampled 3d data using harmonic maps. *International Journal of Computer Vision*, 76(3):283–300, 2008.
- [22] P. Weinzaepfel, J. Revaud, Z. Harchaoui, and C. Schmid. Deepflow: Large displacement optical flow with deep matching. In *Proceedings of the IEEE International Conference on Computer Vision*, pages 1385–1392, 2013.
- [23] R. J. Woodham. Photometric method for determining surface orientation from multiple images. *Optical engineering*, 19(1):191139–191139, 1980.
- [24] L. Yin, X. Chen, Y. Sun, T. Worm, and M. Reale. A high-resolution 3d dynamic facial expression database. In *Automatic Face & Gesture Recognition, 2008. FG'08. 8th IEEE International Conference on*, pages 1–6. IEEE, 2008.
- [25] X. Zhang, L. Yin, J. F. Cohn, S. Canavan, M. Reale, A. Horowitz, P. Liu, and J. M. Girard. Bp4d-spontaneous: a high-resolution spontaneous 3d dynamic facial expression database. *Image and Vision Computing*, 32(10):692–706, 2014.
- [26] X. Zhu, Z. Lei, J. Yan, D. Yi, and S. Z. Li. High-fidelity pose and expression normalization for face recognition in the

wild. In *Proceedings of the IEEE Conference on Computer Vision and Pattern Recognition*, pages 787–796, 2015.

- [27] T. Zinßer, J. Schmidt, and H. Niemann. Point set registration with integrated scale estimation. In *International Conference on Pattern Recognition and Image Processing*, pages 116–119, 2005.